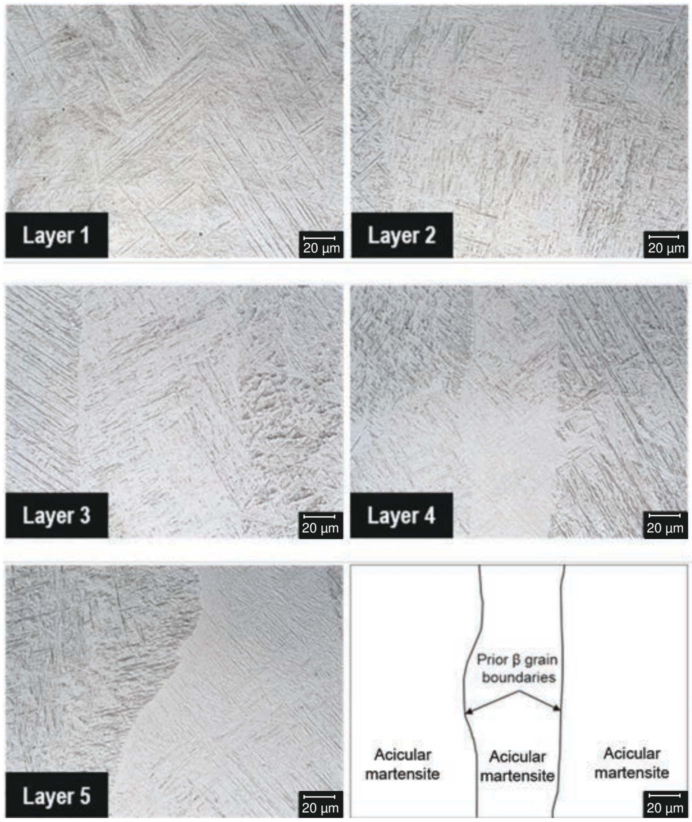

Fig. 22 Micrographs of material representing the first layer after production of five successive layers of Ti-6Al-4V alloy, and a schematic showing the probable phases that have been formed. Source: Ref 18

The complexity of repetitive thermal cycles makes diffusion reaction kinetics difficult to determine accurately, and approaches are being developed to address the nonisothermal nature of these reactions and the combined effect of precipitation kinetics (Ref 33, 34). It should also be noted that complicated scan paths used to produce 3D shapes and changes in heat flow as the build proceeds can result in variability in the thermal response throughout the build geometry, which could influence the local progression and establishment of microstructure. When these aspects of the DED process are combined with the potential for development of aligned microstructures, such as directional solidification of large columnar grains, the possibility exists of variation in microstructure and properties throughout the build and anisotropy of properties based on orientation within the part (Ref 12, 35, 36).

Postprocessing

Postprocessing is usually required to achieve the intended functionality of a part produced by using the DED process, including thermal treatment and thermal treatment with hydrostatic stress (hot isostatic pressing, or HIP), machining, and surface finishing. Because all DED processes inherently create relatively high levels of thermally induced stress during processing, thermal stress relief typically is used after DED. For many alloys, postprocess heat treatment is used to establish a more uniform and appropriate microstructure in the DED-produced material, thus producing greater uniformity of properties throughout the part. Thermal processes include annealing to adjust the phases present or the grain size (to control strength and ductility), solutionizing or solution annealing followed by precipitation or aging treatments to achieve high strength, and postprocess aging to increase strength by growth of precipitates. Controlled environments are used during heat treatment of alloys sensitive to absorption of gaseous species, such as vacuum heat treatment for titanium alloys, or alloys susceptible to elevated-temperature oxidation, such as heat treating tool steels in an inert gas atmosphere. In critical applications requiring minimal potential defects and greater assurance of material quality, HIP is used to close or heal internal defects, such as lack of fusion and porosity, while also adjusting microstructure through heat treatment. In many cases, heat treatment and HIP also serve as thermal stress relief, but part removal from the substrate or base plate, which is typically conducted after stress relief, must also be considered.

This discussion is a general description of potential postprocess heat treatments applicable to material produced by using DED. However, a suitable understanding of the alloy system and established practices is necessary to identify specific postprocess heat treatment for an alloy. Several standards have also been created for guidance and selection of heat treatment practices for additive-manufactured materials (Ref 37). Note that many current heat treatment practices, especially those used for solutionizing, were developed for materials produced by using conventional thermomechanical processing (e.g., casting, elevated-temperature deformation processing, heat treating, and cold working), and times at temperature may not be optimized for addressing microsegregation that could be present in the solidified microstructures of material produced by using DED.

Various methods of postprocess machining and surface finishing are used to prepare DED components and structures for application. While discussion of these processes is not within the scope of this article, several points related to these postprocess operations are appropriate. In many instances, postprocess machining of DED parts is required to achieve geometric dimensions and tolerances as well as the necessary surface condition to meet application requirements, such as for mating surfaces and surfaces for fatigue-critical parts. Sufficient additional material at surfaces to be machined must be incorporated into the build design as an overbuild dimension.

Hybrid additive manufacturing, which combines additive (almost exclusively DED) and subtractive (machining) processing within a single integrated system, is expanding the potential applications for DED. Although hybrid additive manufacturing offers the opportunity for much greater feature resolution and surface finish while delivering higher deposition and production rates characteristic of DED, postprocess thermal treatments are undesirable, because final machining is completed during the DED process. Also, hybrid additive manufacturing of larger components typically uses local shielding instead of processing in a controlled environment. Although the technology offers substantial opportunities for DED, these aspects of hybrid additive manufacturing require close scrutiny of materials selected for processing as well as management of thermal stress that can be generated during processing.

Properties of Metallic Materials Produced by Using Directed-Energy Deposition

Mechanical properties of a material produced by using DED can vary widely based on the process used for deposition, the orientation of the test direction, and the postprocessing applied to the material after deposition. Based on these considerations, reporting test results must include sufficient information that enables establishing the pedigree of the material and process. The static strength of three alloys produced by using various DED processes is presented in Table 4 (Ref 38), which provides minimum

Table 4 Tensile properties of directed-energy deposition (DED)-produced and wrought alloys

Alloy	DED process and feedstock	Condition of material	Specimen orientation	Yield strength		Ultimate tensile strength		Elongation, %	Reference
				MPa	ksi	MPa	ksi		
316L	Wrought plate	Cold finished	Longitudinal	255 min	37 min	525 min	76 min	30 min	39
(S31603)	Laser, powder	DED as-built	*z*	405–415	59–60	620–660	90–96	34–40	42
		DED, heat treated 2 h at 1150 °C (2100 °F), air cooled	*z*	325–355	47–51	600–620	87–90	42–43	
IN-718	Wrought plate	Solution annealed and precipitation hardened	Longitudinal	1034 min	150 min	1275 min	185 min	8 min	40
(N07718)	Laser, powder	DED, heat treated	···	1034	150	1276	185	12	43
	Laser, wire	DED, solution annealed and precipitation hardened	···	1098	159	1321	192	9.8	44
	Electron beam, wire	DED as-built	*x-y*	655	95	978	142	···	45
			y-x	699	101	936	136	···	
		DED, solution annealed and precipitation hardened	*x-y*	986	143	1114	162	···	
			y-x	998	145	1162	169	···	
	Arc, wire	DED as-built	*x-y*	473	69	828	120	28	46
Ti-6Al-4V	Wrought plate	Annealed at 730 °C (1345 °F) for 2 h, air cooled	Longitudinal	827 min	120 min	893 min	130 min	10 min	41
(R56400)	Laser, powder	DED, stress relieved 2 h at 700–730 °C (1290–1345 °F)	*x*	1065	154	1109	161	4.9	47
			y	1066	155	1112	161	5.5	
			z	832	121	832	121	0.8	
		DED, hot isostatic pressed 2 h at 900 °C (1650 °F) and 100 MPa (14.5 ksi)	*x*	946	137	1005	146	13.1	
			y	952	138	1007	146	13.0	
			z	899	130	1002	145	11.8	
	Laser, wire	DED as-built	*x*	1105	160	1163	169	4.0	48
		DED, annealed at 950 °C (1740 °F)	*x*	975	141	1053	153	7.5	
	Electron beam, wire	DED, stress relieved 2 h at 650 °C (1200 °F)	*z*	839	122	930	135	16.5	49(a)

(a) Data represent an average of 26 specimens in the *z*-direction, which were produced by using a power of 8.5 kW and a deposition rate of 6.9 kg/h (15.2 lb/h). Source: Ref 38

properties for 316L (UNS S31603), IN-718 (UNS N07718), and Ti-6Al-4V (UNS R56400) wrought products (Ref 39–41) as well as reported properties of these alloys produced by using several DED techniques and representing as-built and postprocess heat treated conditions (Ref 42–49). It should be noted that these data are presented for initial comparative purposes and are not sufficient to provide a statistical basis for expected properties.

An important aspect of the data is the potential of material produced using the DED process to achieve strength comparable to its wrought counterpart, and these data suggest that strength can be achieved for the alloys described in the table, depending on the DED process and post-processing. As discussed previously, the resultant microstructure—and mechanical properties associated with the microstructure—for material produced by the DED process is dependent on processing and postprocessing conditions. The data in Table 4 also show the effect of postprocess heat treatment compared with as-built material. This is especially true for alloys that react metallurgically to thermal treatments for increasing strength, such as IN-718, which was designed to respond to solution annealing and precipitation strengthening. Processing conditions can also influence mechanical properties. The potential for preferential grain growth in the direction of the build (*z*-orientation) can also affect strength. This is illustrated by the data for Ti-6Al-4V in Table 4. In this case, tensile strength in the *z*-orientation is lower than material tested in the *x*- or *y*-orientations, which represents material in the horizontal plane of the build (Ref 50). The data in Table 4 are intended to reinforce the importance of process and processing conditions on the strength of material produced by DED. These results illustrate the significant variation of tensile strength based on the process, postprocessing, and test orientation of IN-718 and Ti-6Al-4V alloys.

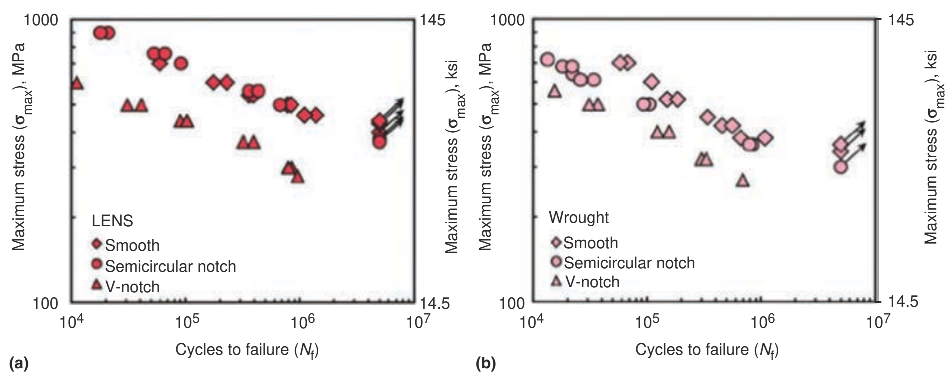

Fig. 23 Results of high-cycle fatigue tests for Ti-6Al-4V alloy representing smooth and notched specimens taken from (a) stress-relieved laser-based directed-energy deposition material in the *z*-orientation and (b) mill-annealed plate. LENS, laser-engineered net shaping. Source: Ref 51

Data from Razavi and Berto (Ref 51) shown in Fig. 23 describe results of high-cycle fatigue in terms of maximum stress and cycles to failure under axial loading ($R = 0.01$ and $f = 10$ Hz) for wrought and DED-produced material for Ti-6Al-4V. The DED specimens, representing the *z*-orientation, were produced using powder feedstock, with a postprocess stress relief at 600 °C (1110 °F) for 1 h followed by air cooling, and machined to produce smooth, notched geometries. Wrought specimens were taken from plate in the mill-annealed condition and machined to produce smooth, notched geometries. Test results indicate that fatigue performance of smooth, semicircular-notched DED and wrought specimens was similar, with DED material outperforming wrought material in some cases, which was believed to be due to the finer grain size in the DED material. However, DED material did not perform as well as wrought material in V-notched specimens, which was attributed to a smaller region of material at the crack tip exhibiting fewer grains having favorable grain orientation for crack initiation. Although grain size and orientation undoubtedly impact fatigue performance, the potential presence of small internal defects, such as lack of fusion, unmelted powder, and pores, can also influence fatigue (Ref 52). This was substantiated by evaluations regarding the use of postprocess HIP to reduce internal defects for improved fatigue performance of Ti-6Al-4V (Ref 53–55).

Research is underway to better understand the development of microstructure and resultant mechanical properties for the various alloys and processes being used for additive manufacturing. This work is not only addressing the need for additional data concerning the numerous static and dynamic mechanical properties required for designing engineered components but is also directed at other properties and attributes, such as corrosion resistance, electrical and thermal conductivity, and machinability, to name a few. In all cases, the need to closely control and document all aspects of the additive manufacturing process is necessary to completely define the material representing these properties.

Unique Materials for Directed-Energy Deposition

The various DED processes are also being applied to a wide variety of unique materials, and, in many instances, the deposition and establishment of distinctive properties in these materials are taking advantage of the inherent attributes of the process (Ref 56). This can include the use of high-energy vacuum processing, electron-beam-based DED for producing components in reactive and refractory metals (Ref 57), and using the high solidification and cooling rates of laser-based DED for surface deposition on a component by using metal alloys that exhibit amorphous characteristics (Ref 58).

One category of unique materials produced by using the DED process that have been adopted for use in commercial applications is metal-matrix composites (MMCs) produced by using laser-based deposition, primarily to impart improved wear resistance on the surface of components. This technique uses a powder blend consisting of a matrix alloy and hard particles. One of the first applications involved the use of nickel-base alloys as the matrix material, with tungsten carbide (WC) reinforcing particles (Ref 59). The blend was found experimentally to enable the WC to remain relatively stable and not dissolve in the nickel-base alloy molten pool, thus providing a composite structure having hard particles in a ductile matrix. The use of thermodynamic analysis to predict phase stability of a matrix alloy with other hard-particle systems has been applied to the development of a martensitic stainless steel alloy matrix containing titanium carbide (TiC) particles (Ref 15, 60). Other MMC systems are being developed for DED to locally enhance properties and characteristics of components through the use of advanced deposition materials (Ref 61, 62).

Applications for Directed-Energy Deposition Processes

The use of DED is rapidly expanding, based on greater acceptance of these processes as a reliable industrial practice and awareness of the benefits of this additive manufacturing technology. Applications are being developed for DED processes in the aerospace, energy, defense, and automotive industries, including the use of DED processing for selective deposition on existing and new components to impart improved surface characteristics and to create near-net and net-shaped parts.

Selective Deposition by Using Directed-Energy Deposition

All DED processes have been used to selectively add material onto an existing component to restore geometric dimensions and to locally enhance certain characteristics at the surfaces of interest. In the case of restoration of dimensions, the material added can be the same alloy as that of the component or a different alloy that is compatible with the base alloy and provides properties and characteristics similar to those of the existing component. Metallurgical compatibility between the added material and the underlying substrate plays an important role in selection. Metallurgical compatibility is usually governed by the propensity of the deposit or underlying material to crack during or after solidification, which is strongly influenced by the new composition created from the alloy addition and the amount of material melted from the substrate. This is the same consideration when selecting a filler metal during welding. However, the refined microstructure and compressive stress resulting from high solidification rates exhibited in many DED processes provide greater freedom to select an alloy for deposition. Also, the original surface of the component may have been treated to improve surface characteristics, such as chromium electroplating and surface nitriding, and these processes can hinder the ability to create defect-free deposits. Under these conditions, the original surface treatment must be removed prior to deposition.

For many materials, such as medium-carbon steels, austenitic stainless steels, nickel-base alloys, and titanium alloys, the alloy used for the DED process can be identical to the alloy of the component. However, when the component is produced from a material that could be sensitive to cracking, a more compatible alloy can be used for deposition. Examples include the use of an aluminum alloy for repair that is less prone to solidification cracking than the component alloy, and the application of a cobalt-chromium alloy onto a high-alloy steel to restore a part requiring high hardness.

For DED processes used to enhance local surface characteristics, the material added is selected based on the performance requirements of the component. The majority of these applications are for improving wear resistance and corrosion resistance at the surface, and, in some cases, both are required. Materials used extensively in these applications include cobalt-chromium alloys, nickel-base alloys, and martensitic stainless steels; examples for each system are shown in Table 1.

Examples of using DED to selectively add material to the surface of existing or new components are shown in Fig. 24 to 26. In Fig. 24, laser-based DED is used to add bosses along a stainless steel cylindrical component used as a directional drill bit for the oil and gas industry. After deposition, the part is milled for insertion of embedded sensors. An initial layer of

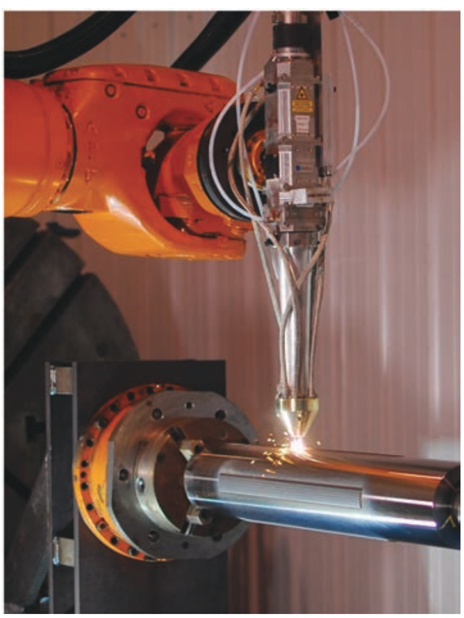

Fig. 24 Image of laser-based directed-energy deposition process for selectively adding features to a cylindrical component. Courtesy of Synergy Additive Manufacturing LLC

Fig. 25 Image of laser-based directed-energy deposition process for depositing a wear-resistant material onto the surface of a large die. Courtesy of Alabama Laser

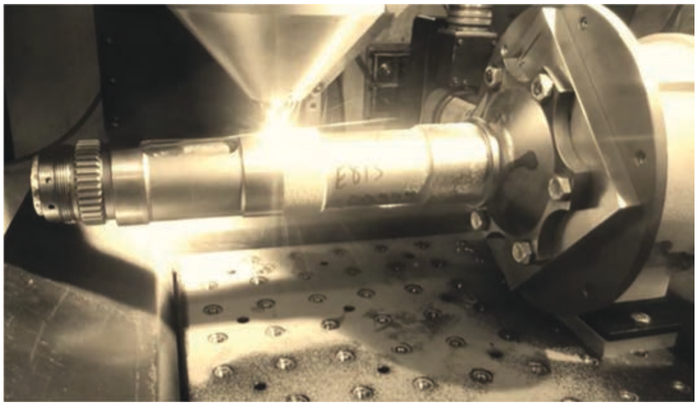

Fig. 26 Image of laser-based directed-energy deposition process used to restore geometric dimensions on a titanium shaft. Courtesy of the Center for Innovative Materials Processing through Direct Digital Deposition, Pennsylvania State University

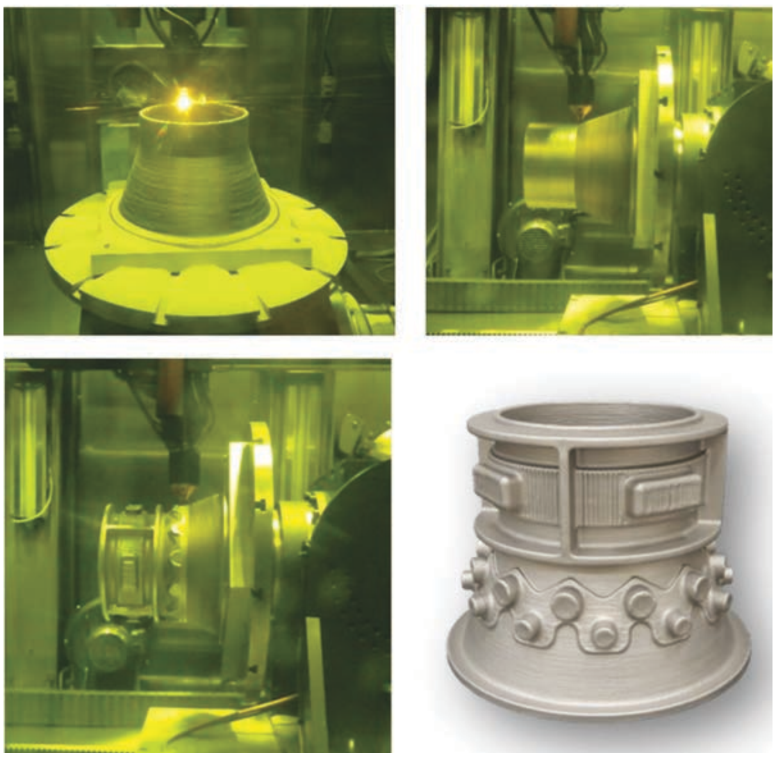

Fig. 27 Images of laser-based directed-energy deposition system applied to produce a complex IN-718 alloy casing, which is also shown in the completed near-net form. Courtesy of RPM Innovations

IN-625 alloy was deposited as a buffer for the base alloy; subsequent layers were added by using a powder blend of IN-625 with spherical WC particles to impart high wear resistance. Figure 25 shows laser-based deposition of a wear-resistant alloy onto strategic areas of a large die to help extend its useful life. Life extension through refurbishment provides significant cost-savings compared with the cost of a new die. Figure 26 shows a laser-based DED process used to deposit Ti-6Al-4V material onto the surface of a Ti-6Al-4V shaft to restore critical dimensions in worn bearing areas. Low energy was used to minimize thermal distortion of the part. The hardness of the deposition material matched the substrate hardness, and there was no change in shaft diameter and concentricity from DED processing.

Producing Shapes by Using Directed-Energy Deposition

Opportunities for applying DED processes are growing rapidly. In the case of DED, many applications are taking advantage of decreased processing time through higher deposition rates, increased build envelope, and the potential for multiple material processing. This is especially true for electron-beam-based DED, which has the additional value of operating in a vacuum environment to process reactive materials that could be sensitive to low levels of contamination. Although DED is considered an additive manufacturing process capable of high production rates at the cost of feature quality (e.g., for producing near-net shapes), the introduction of hybrid additive manufacturing that combines additive (deposition) processing with subtractive (machining) technology within an integrated system expands the capability of DED to produce larger formats and net shape quality.

Figure 27 shows the use of a laser-based DED process to create a complex 400 mm (16 in.) diameter near-net shape IN-718 casing, which underwent postprocess thermal treatment and machining. Deposition was conducted in an argon atmosphere using five axes of motion. The main wall of the casing was built by using rotation, and a combination of rotation and tilt was used to achieve complex motion to produce overhanging features without the need of support structures. Figure 28 shows an example of using the electron-beam-based DED process to produce a large near-net shape Ti-6Al-4V component during deposition, the near-net shape after deposition, and the completed structure after machining. The DED process was selected to demonstrate the potential for achieving high-quality parts and reducing cost by decreasing the required amount of material, compared with using traditional machining to form the part. The electron-beam-based process is especially applicable to titanium alloys, due to processing in a vacuum to control oxygen levels within the deposit. The use of hybrid processing is shown in Fig. 29, combining a laser-based DED process with a full range of machining capabilities to produce net shape components. The process shown in the figure uses five axes of motion, with the ability of the machine turret to exchange deposition heads and multiple machining tools to produce relatively large, complex parts.

As the benefits of DED become apparent to industry, the use of DED processes will continue to grow. The potential advantages of DED in shortening the manufacturing cycle, reducing cost in time and materials, recouping high-value components through repair, offering increased product performance through unique designs, and incorporating multiple materials will spur further application of the technology. While DED offers considerable promise, areas of technology and support that will help enable the growth and bring the processes for industrial applications to maturity include application of advanced sensing techniques coupled with improved data and process analysis to assist in increasing DED reliability, and the coordinated collection of mechanical property data for materials produced to establish expected properties needed for design.

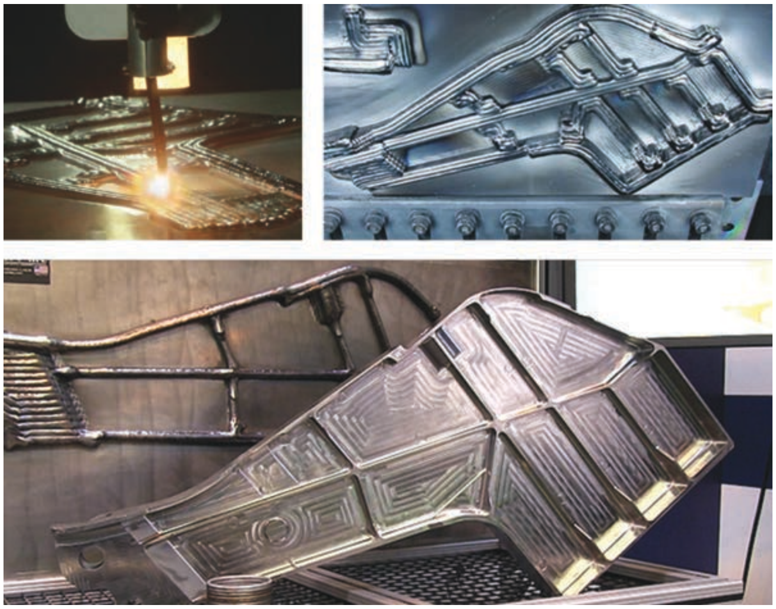

Fig. 28 Images of electron-beam-based directed-energy deposition of Ti-6Al-4V alloy during deposition, the completed near-net shape, and the final structure after machining. Courtesy of Sciaky Inc.

Fig. 29 Illustration of applying a hybrid process using laser-based directed-energy deposition and five axes of machining in a single integrated process. Courtesy of DMG Mori

REFERENCES

1. K.H. Leong and B.V. Hunter, Improving Fiber-Optic Laser Beam Delivery by Incorporating GRADIUM Optics, *Appl. Optics*, Vol 36, 1997, p 2763
2. Industrial Robot Axes Illustration (Drawing), Aaltomies, 2016, https://aaltomies.files.wordpress.com/2016/03/industrial-robot-axes-illustration1.jpg (accessed June 2019)
3. R.P. Martukanitz, R.M. Melnychuk, and S. M. Copley, Dynamic Absorption of a Powder Layer, *Proceedings of the 23rd International Congress of Applications of Lasers and Electro-Optics,* Laser Institute of America, 2004, p 1404–1409
4. T. DebRoy and S. Kou, Heat Flow in Welding, *Welding Handbook*, Vol 1, 9th ed., American Welding Society, 2001, p 87
5. F. Lia, J. Parks, J. Tressler, and R. Martukanitz, Partitioning of Laser Energy during the Directed Energy Deposition Process, *J. Add. Manuf*., Vol 18, 2017, p 31
6. M.N. Ahsan and A.J. Pinkerton, An Analytical-Numerical Model of Laser Direct Metal Deposition Track and Microstructure Formation, *Model. Simul. Mater. Sci. Eng*., Vol 19, 2011, p 055003
7. S. Kelly, "Development of Repair Procedures for Ti-6Al-4V Alloy," Technical Memorandum, Applied Research Laboratory, Pennsylvania State University, 2011
8. N.S. Bailey, C. Katinas, and Y.C. Shin, Laser Direct Deposition of AISI H13 Tool Steel Powder with Numerical Modeling of Solid Phase Transformation, Hardness, and Residual Stresses, *J. Mater. Process. Technol*., Vol 247, 2017, p 223–233, https://doi.org/10.1016/j.jmatprotec.2017.04.020
9. W. Wang, A.J. Pinkerton, L.M. Wee, and L. Li, Component Repair Using Laser Direct Metal Deposition, *Proceedings of the 35th International MATADOR Conference*, Springer, London, 2007, https://doi-org.proxy01.its.virginia.edu/10.1007/978-1-84628-988-0_78
10. L. Xue, J. Chen, and S.H. Wang, Freeform Laser Consolidated H13 and CPM 9V Tool Steels, *Metallogr. Microstruct. Anal*., Vol 2, 2013, p 67–78, https://doi-org.proxy01.its.virginia.edu/10.1007/s13632-013-0061-0
11. P. Kattire, S. Paul, R. Singh, and W. Yan, Experimental Characterization of Laser Cladding of CPM 9V on H13 Tool Steel for Die Repair Applications, *J. Manuf. Process*., Vol 20, 2015, p 492–499
12. E. Bassoli, L. Denti, A. Gatto, R. Emilia, and N.T. Sewell, Directed Energy Deposition of Steel 316L: Effects of Build Orientation, *Int. J. Mech. Eng. Technol*., Vol 9 (No. 8), Aug 2018, p 438–446
13. F.M. Sciammarella and B.S. Najafabadi, Processing Parameter DOE for 316L Using Directed Energy Deposition, *J. Manuf. Mater. Process*., Vol 2, 2018, p 61
14. M.A. Melia, H.A. Nguyen, J.M. Rodelas, and E.J. Schindelholz, Corrosion Properties of 304L Stainless Steel Made by Directed Energy Deposition Additive Manufacturing, *Corros. Sci*., Vol 152, 2019, p 20–30
15. R.P. Martukanitz and S.S. Babu, Development of Advanced Coatings for Laser Modifications through Process and Materials Simulation, *Proceedings of the International Conference on Materials Processing and Design: Modeling, Simulation, and*

Applications, American Institute of Physics, 2004, p 1539–1546

16. J.X. Fang, S.Y. Dong, Y.J. Wang, B.S. Xu, Z.H. Zhang, D. Xia, W.B. Ren, and P. He, Microstructure and Properties of an As-Deposited and Heat Treated Martensitic Stainless Steel Fabricated by Direct Laser Deposition, *J. Manuf. Process.*, Vol 25, 2017, p 402–410
17. N.K. Adomako, S. Noh, C.S. Oh, S. Yang, and J.H. Kim, Laser Deposition Additive Manufacturing of 17-4PH Stainless Steel on Ti-6Al-4V Using V Interlayer, *Mater. Res. Lett.*, 2019, p 259–266
18. F. Lia, J.Z. Park, J.S. Keist, S.B. Joshi, and R. Martukanitz, Thermal and Microstructural Analysis of Laser-Based Directed Energy Deposition for Ti-6Al-4V and Inconel 625 Deposits, *Mater. Sci. Eng. A*, Vol 717, 2018, p 1–10, https://doi.org/10.1016/j.msea.2018.01.060
19. G.P. Dinda, A.K. Dasgupta, and J. Mazumder, Laser Aided Direct Metal Deposition of Inconel 625 Superalloy: Microstructural Evolution and Thermal Stability, *Mater. Sci. Eng. A*, Vol 509, 2009, p 98–104
20. B. Chen and J. Mazumder, Role of Process Parameters during Additive Manufacturing by Direct Metal Deposition of Inconel 718, *Rapid Prototyp. J.*, Vol 23, 2017, p 919–929
21. Y.N. Zhang, X. Cao, P. Wanjara, and M. Medraj, Fiber Laser Deposition of Inconel 718 Using Powders, *Materials Science and Technology Conference and Exhibition 2013 (MS&T 2013)*, Vol 1, 2013, p 37–49
22. A. Saboori, D. Gallo, S. Biamino, P. Fino, and M. Lombardi, An Overview of Additive Manufacturing of Titanium Components by Directed Energy Deposition: Microstructure and Mechanical Properties, *Appl. Sci.*, Vol 7, 2017, p 883
23. B. Dutta and F. Froes, The Additive Manufacturing (AM) of Titanium Alloys, *Met. Powder Rep.*, Vol 72, 2017, p 96–106
24. B. Baufeld, T. Dutilleul, and R. Widdison, "Wire Based Electron Beam Additive Manufacturing," 70th IIW Annual Assembly and International Conference (Shanghai, China), 2018
25. S. Lathabai, Fundamentals of Aluminium Metallurgy—Recent Advances, *Additive Manufacturing of Aluminium-Based Alloys and Composites*, Woodhead Publishing Series in Metals and Surface Engineering, 2018, p 47–92
26. J.H. Martin, B.D. Yahata, J.M. Hundley, J. A. Mayer, T.A. Schaedler, and T.M. Pollock, 3D Printing of High-Strength Aluminium Alloys, *Nature*, Vol 549, 2017, p 365–369
27. F. Caiazzo and V. Alfieri, Simulation of Laser-Assisted Directed Energy Deposition of Aluminum Powder: Prediction of Geometry and Temperature Evolution, *Materials*, Vol 12, 2019, p 2100
28. R. Singh, D. Kumar, S.K. Mishra, and S. K. Tiwari, Laser Cladding of Stellite 6 on Stainless Steel to Enhance Solid Particle Erosion and Cavitation Resistance, *Surf. Coat. Technol.*, Vol 251, 2014, p 87–97
29. Y.P. Kathuria and A. Tsuboi, Laser Cladding of Stellite #6: A Detailed Analysis, *Proceedings of Lasers, Optics, and Vision for Productivity in Manufacturing I* (Besancon, France), 1996, https://doi.org/10.1117/12.251166
30. X. Zhang, W. Cui, W. Li, and F. Liou, Effects of Tool Path in Remanufacturing Cylindrical Components by Laser Metal Deposition, *Int. J. Adv. Manuf. Technol.*, Vol 100, 2019, p 1607–1617, https://doi.org/10.1007/s00170-018-2786-z
31. F. Lia, J. Park, J. Tressler, and R. Martukanitz, Laser Beam-Material Interaction and Thermal Absorption Model Validation, *Materials Science and Technology Conference and Exhibition 2014 (MS&T 2014),* Vol 18, p 2019–2036
32. S. Kou, *Welding Metallurgy*, 2nd ed., John Wiley, Inc., 2002
33. S.M. Kelly and S.L. Kampe, Microstructural Evolution in Laser-Deposited Multilayer Ti-6Al-4V Builds, Part II: Thermal Modelling, *Metall. Mater. Trans. A*, Vol 35, 2004, p 1869–1879, https://doi.org/10.1007/s11661-004-0095-7
34. A. Crespo and R. Vilar, Finite Element Analysis of the Rapid Manufacturing of Ti-6Al-4V Parts by Laser Powder Deposition, *Scr. Mater.*, Vol 63, 2010, p 140–143
35. N.A. Kistler, D.J. Corbin, A.R. Nassar, E. W. Reutzel, and A.M. Beese, Effect of Processing Conditions on the Microstructure, Porosity, and Mechanical Properties of Ti-6Al-4V Repair Fabricated by Directed Energy Deposition, *J. Mater. Process. Technol.*, Vol 264, 2019, p 172–181
36. S. Wolff, T. Lee, E. Faierson, K. Ehmann, and J. Cao, Anisotropic Properties of Directed Energy Deposition (DED)-Processed Ti-6Al-4V, *J. Manuf. Process.*, Vol 24, 2016, p 397–405, https://doi.org/10.1016/j.jmapro.2016.06.020
37. SAE International, http://profiles.sae.org/teaamsam-m/ (accessed July 2019)
38. J.J. Lewandowski and S. Mohsen, Metal Additive Manufacturing: A Review of Mechanical Properties, *Annu. Rev. Mater. Res.*, Vol 46, 2016, p 151–186, https://doi.org/10.1146/annurev-matsci-070115-032024
39. D. Benjamin and C.W. Kirkpatrick, Ed., *Properties and Selection: Stainless Steels, Tool Materials, and Special-Purpose Metals*, Vol 3, *Metals Handbook*, 9th ed., American Society for Metals, 1980, p 113–121
40. "Standard Specification for Precipitation-Hardening Nickel Alloy (UNS N07718) Plate, Sheet, and Strip for High-Temperature Service," B 670-07, ASTM International, 2018
41. "Standard Specification for Titanium and Titanium Alloy Strip, Sheet, and Plate," B 265 6Al-4V Grade 5, ASTM International
42. A. Yadollahi, N. Shamsaei, S.M. Thompson, and D.W. Seely, Effect of Process Time Interval and Heat Treatment on the Mechanical and Microstructural Properties of Direct Laser Deposited 316L Stainless Steel, *Mater. Sci. Eng. A*, Vol 644, 2015, p 171–183
43. H. Qi, M. Azer, and A. Ritter, Studies of Standard Heat Treatment Effects on Microstructure and Mechanical Properties of Laser Net Shape Manufactured Inconel 718, *Metall. Mater. Trans. A*, Vol 40, 2009, p 2410–2422
44. Y. Zhang, X. Cao, P. Wanjara, and M. Medraj, Tensile Properties of Laser Additive Manufactured Inconel 718 Using Filler Wire, *J. Mater. Res.*, Vol 29, 2014, p 2006–2020
45. W.A. Tayon, R.N. Shenoy, M.R. Redding, R.K. Bird, and R.A. Hafley, Correlation between Microstructure and Mechanical Properties in a Inconel 718 Deposit Produced via Electron Beam Freeform Fabrication, *J. Manuf. Sci. Eng.*, Vol 136, 2014, p 061005
46. B. Baufeld, Mechanical Properties of Inconel 718 Parts Manufactured by Shaped Metal Deposition (SMD), *J. Mater. Eng. Perform.*, Vol 21, 2012, p 1416–1421
47. P.A. Kobrym and S.L. Semiatin, Mechanical Properties of Laser-Deposited Ti-6Al-4V, *Proceedings of the Solid Freeform Fabrication Conference 2001* (University of Texas), p 179–186
48. G.P. Dinda, L. Song, and J. Mazumder, Fabrication of Ti-6Al-4V Scaffolds by Direct Metal Deposition, *Metall. Mater. Trans. A*, Vol 39, 2008, p 2914–2922
49. R. Salo, Sciaky Inc., personal communication, Aug 2019
50. J.S. Keist and T.A. Palmer, Role of Geometry on Properties of Additively Manufactured Ti-6Al-4V Structures Fabricated Using Laser Based Directed Energy Deposition, *Mater. Des.*, Vol 106, 2016, p 482–494
51. M. Razavi and F. Berto, Directed Energy Deposition versus Wrought Ti-6Al-4V: A Comparison of Microstructure, Fatigue Behavior, and Notch Sensitivity, *Adv. Eng. Mater.*, 2019, 10.1002/adem.201900220
52. S.M.J. Razavi, G.G. Bordonaro, P. Ferro, J. Torgersen, and F. Berto, Fatigue Behavior of Porous Ti-6Al-4V Made by Laser-Engineered Net Shaping, *Materials,* Vol 11, 2018, 10.3390/ma11020284
53. S. Tammas-Williams, P.J. Withers, I. Todd, et al., The Effectiveness of Hot Isostatic Pressing for Closing Porosity in Titanium Parts Manufactured by Selective

Electron Beam Melting, *Metall. Mater. Trans. A*, Vol 47, 2016, p 1939, https://doi.org/10.1007/s11661-016-3429-3

54. M.-W. Wu, J.-K. Chen, B.-H. Lin, and P.-H. Chiang, Improved Fatigue Endurance Ratio of Additive Manufactured Ti-6Al-4V Lattice by Hot Isostatic Pressing, *Mater. Des.*, Vol 134, 2017, p 163–170
55. A. Yadollahi and N. Shamsaei, Additive Manufacturing of Fatigue Resistant Materials: Challenges and Opportunities, *Int. J. Fatigue*, Vol 98, 2017, p 14–31
56. A. Dass and A. Moridi, State of the Art in Directed Energy Deposition: From Additive Manufacturing to Materials Design, *Coatings*, Vol 9, 2019, p 418, 10.3390/coatings9070418
57. J. Johnson and T. Palmer, Directed Energy Deposition of Molybdenum, *Int. J. Refract. Met. Hard Mater.*, 2019, p 105029
58. S. Su and Y. Lu, Laser Directed Energy Deposition of Zr-Based Bulk Metallic Glass Composite with Tensile Strength, *Mater. Lett.*, Vol 247, 2019, p 79–81
59. K. Van Acker, D. Vanhoyweghen, R. Persoons, and J. Vangrunderbeek, Influence of Tungsten Carbide Particle Size and Distribution on the Wear Resistance of Laser Clad WC/Ni Coatings, *Wear*, Vol 258, 2005, p 194–202
60. S.S. Babu, R.P. Martukanitz, K.D. Parks, and S.A. David, Toward Prediction of Microstructural Evolution during Laser Surface Alloying, *Metall. Mater. Trans. A*, Vol 33, 2002, p 1189–1200
61. P.K. Farayibi, T.E. Abioye, A. Kennedy, and A.T. Clare, Development of Metal Matrix Composites by Direct Energy Deposition of “Satellited” Powders, *J. Manuf. Process.*, Vol 45, 2019, p 429–437
62. O. Oyelola, P. Crawforth, R. M’Saoubi, and A.T. Clare, Machining of Functionally Graded Ti-6Al-4V/WC Produced by Directed Energy Deposition, *Add. Manuf.*, Vol 24, 2018, p 20–29

ASM Handbook, Volume 24, *Additive Manufacturing Processes*
D. Bourell, W. Frazier, H. Kuhn, M. Seifi, editors
DOI 10.31399/asm.hb.v24.a0006569

Binder Jetting and Sintering in Additive Manufacturing

Amy Elliott, Corson Cramer, Peeyush Nandwana, Oak Ridge National Laboratory

ENCOMPASSED IN THE FIELD of additive manufacturing (AM) is a variety of layer-wise manufacturing machines that use a wide range of feedstock, deposition, and densification technologies (Ref 1). Unlike the well-known laser technologies, binder jetting is a powder bed-based additive manufacturing technology that, in combination with inkjet technology, produces bound-powder parts (aka "green" parts) that can be densified in a variety of ways (Ref 2). Most commonly, the bound powder parts are infiltrated with either a metal or polymer to give the printed parts mechanical integrity (Ref 3). However, modern techniques focus on densifying the bound powder parts completely to form fully dense, single alloy (metal) artifacts very similar to the technique used in metal injection molding (MIM) (Ref 4, 5). Although many other variations and use cases for binder jetting exist, such as prototyping with printed gypsum (Ref 6) and plastic powder shaping with HP's binder jet/powder bed fusion hybrid system (Ref 7), this article focuses on binder-jetting technologies that produce metal artifacts either directly or indirectly. The intent is not to avoid discussing binder jetting of plastics, minerals, and other nonmetals, but rather to focus on the most strategic and widespread uses of the technology.

Binder jet technology is experiencing increasing attention from manufacturing industries due to its low cost/high productivity status compared with laser powder bed fusion (Ref 8–10) and its potential to produce a variety of high-resolution (Ref 11), single-material components with near-isotropic properties (Ref 12). In terms of metal parts, binder jetting has produced more metal AM parts than any of the other AM processes combined (ExOne has been producing metal parts for Shapeways for years, for example (Ref 13)). However, as an "indirect" AM process with the stigma associated with the depowdering and sintering process, binder jetting has lacked significant research support compared with direct metal technologies such as laser and electron beam. These negative stereotypes are slowly being overcome by demonstrations in MIM-replacement production by ExOne and Digital Metal (Ref 13, 14) However, many fundamental challenges still await those who seek to expand the technology to larger print sizes and new industry-grade materials (Ref 15–17). This article reviews some of the challenges and opportunities for binder jetting technology.

History of Binder Jetting

Binder jetting has a history that dates to the early 1990s in a small lab at Massachusetts Institute of Technology (MIT) (Ref 18). The inventors may have first used the technology as a "parlor trick," by taking powdered sugar and binding it layer by layer into intricate shapes to create elaborate "sugar cube" creations for sweetening beverages in style. The first endeavor to commercialize the technology came from the spinoff company Z Corp., which used a type of powdered gypsum as a printing medium and a glucose-water mixture as a binder (Ref 19). The technology was a welcomed improvement from the very first AM technology, stereolithography, which produced parts that sagged over time and only came in an unattractive amber color. By using the multicolor ability of standard inkjet printing technology, Z Corp. machines could produce elaborate objects in full color. However, the fragility of the parts reinforced the classification of these early AM technologies as "rapid-prototyping" techniques rather than the manufacturing process they would later become. As the identity of binder jetting evolved, it became known by different terms such as 3D printing, and as other technologies emerged, it was specified as "indirect 3D printing." ASTM Committee F42 finally settled on binder jetting, which differentiates the technology from powder bed fusion and material jetting, as well as the seven other AM technologies.

In the background of Z Corp.'s success, patents for the technology were filed around printing metal powders that could be brazed or infiltrated with other metals to reach full density, and, therefore, reasonable mechanical properties (Ref 20, 21). The patents were acquired by Extrude Hone, a company in Pennsylvania, which later was split from Extrude Hone and renamed ExOne. ExOne produced bronze-steel parts for decades using binder jetting and is a world leader in metal additive manufactured parts. The company produces hundreds of thousands of parts per year for service bureaus such as Shapeways (Ref 22). With the expiration of the MIT Patents, other companies are entering the market with new binder-jet systems, such as Desktop Metal, Digital Metal, HP, and GE (Ref 23–26). These events, together with the recognition of binder jetting as a viable metal additive manufacturing technology, have led to the expansion of binder jet machine design space and pushed the boundaries in material selection for binder jet prints. Binder jetting is growing at a rapid pace and is poised to become the leader among metal AM technologies.

The most recent revolution in binder jetting focuses on fully dense single alloys; i.e., reaching full density without infiltration to produce single-alloy artifacts with mechanical properties of the base alloy. Through careful selection of powder feedstock and furnace cycles, the driving forces of sintering can be leveraged to draw the loosely bound particles of the preform together, shrinking the object into a smaller, but fully dense version of the print. Currently, small fully dense stainless steel parts are being demonstrated on a size scale similar to that for MIM (Ref 22). This strategy is limited in size due to distortion during the shrinking process, which is discussed later in this article.

Overview of Binder Jetting Process

The major steps of the binder jet process (Fig. 1) are:

1. Printing in the powder bed
2. Curing in a low-temperature oven

3. Depowdering
4. Sintering/postprocessing

Printing involves the deposition of binder into the powder bed layer by layer. The result is basically a box of powder with binder arranged in the shape of the 3D design files. At this point, the binder is still wet, and the parts in the powder bed are malleable like wet clay. After the print is completed, traditional binder systems require a curing step, in which the entire build volume is removed from the printer and heated to a temperature around 200 °C (390 °F) in a curing oven to boil off the solvent carrier in the binder system. The curing step is a hands-off process, which usually takes place overnight in a programmed oven. After parts are fully cured and cooled to handling temperatures, the next step is depowdering, in which individual powder prints are removed from the powder bed, brushed, and blown off. At this stage, the part comprises loosely bound powder (usually about 50% dense) with very low mechanical strength. To reach usable mechanical properties, the void space in the part must be either eliminated by sintering or filled by infiltration with another material. Therefore, the final step is to process the parts in a furnace. Parts are prepared by placing them in a crucible with some other components like infiltration runners or sintering setters.

After removing infiltrated parts from the furnace, their runners are removed, and they can be tumble polished to improve surface finish and inspected for quality. Each major step is discussed in detail in the following sections.

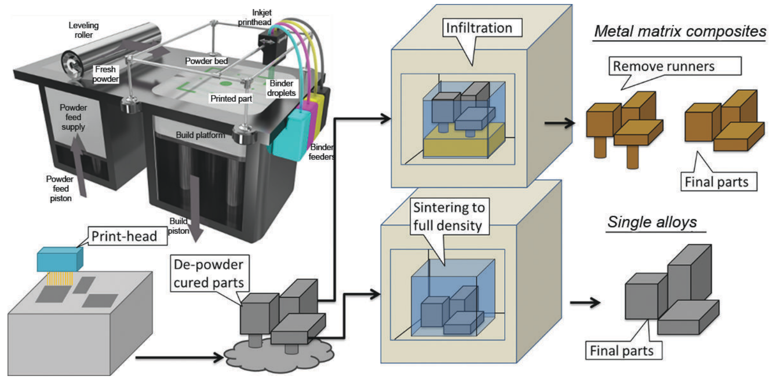

Fig. 1 Binder-jet process cycle. Top left image from Ref 27. Other images adapted from Ref 28.

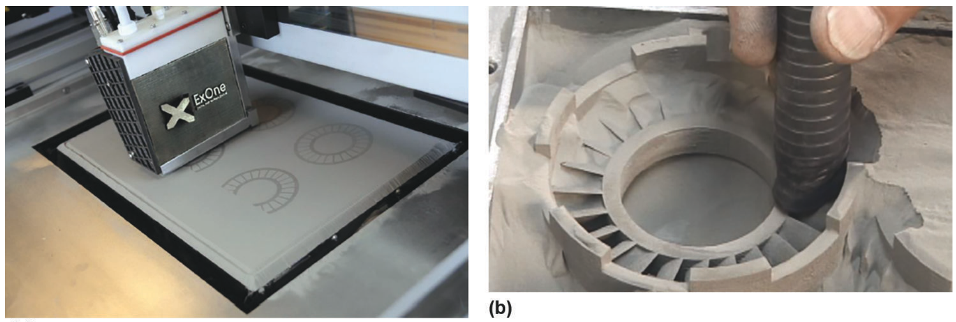

(a) (b)

Fig. 2 (a) Image of a layer of powder in mid-print in the binder jet process and (b) depowdering after the curing step. Source: Ref 29

Printing

As previously mentioned, the binder jet printing process works by spreading layers of powder and ink-jetting binder into each layer to create a loosely bound powder preform (Fig. 2a). Although the printing step seems simple, there are many motions involved in preparing the print layer and managing the inkjet system during printing. Compared with extrusion AM, which requires only a gantry and nozzle, binder-jetting machines have a significant number of components to make the process work. In terms of mechanisms, the major components of a binder-jet system are:

- Build box
- Build stage/Z axis
- Powder hopper/storage
- Powder dispenser
- Powder spreader
- Printhead
- Binder storage
- Heater
- Gantries for powder and printhead

One can start at the center of the action (the build area) when going through the different system components. The build area consists of the build box with an inner stage known as the build plate, build stage, or, as referred to by most operators, the Z axis. The build stage is the level surface that the powder rests on as the layers of the build are deposited. With each new layer, the build plate lowers into the build box via actuation by the Z-axis system, dropping deeper and deeper into the build box (and further away from the print-head). It should be noted that the build stage is different from a starting plate, which is used in powder bed fusion, in that the build stage in binder jetting is not used to anchor the prints nor is it always removed from the build box after printing is complete. Therefore, the binder jet build stage is not a consumable as it is in powder bed fusion.

To begin the print, powder is dispensed from the holding container. With a hopper system, powder is held above the build area and is gravity fed into a dispensing mechanism or "recoater," which deposits the material on top of the build area. Other methods for dispensing powders can be used (such as a feed area that moves in reverse of the build area by pushing material upward and into the path of the roller), but the hopper and recoater system is the most common. After the powder is dispensed, it is pushed from one side to the other by a powder spreading mechanism, which is typically a counter-rotating roller (CRR). CRRs are much better for powder packing than wiper blades or combs used in powder bed fusion, because they create more movement in the powder (Ref 30). While they are ideal for binder jetting, CRRs are not usually used in powder bed fusion, because the welding during printing can create raised features that can damage a roller. CRRs give binder jetting a major advantage over powder bed fusion systems in that numerous different powder shapes and sizes can be spread with ease.

After the layer of powder is dispensed and spread, binding of the layer proceeds. To deposit the binder, an inkjet printhead passes over the layer and deposits discrete drops of binder over the powder in the shape of the 2D cross section of the part. Because the printhead can have up to 1000 individual nozzles, high volumes of binder can be deposited with high accuracy, meaning the layer can be completed quickly without sacrificing quality. After impact with the powder, binder droplets wick downward and outward into the powder until it reaches equilibrium, establishing the 3D "voxels" of the part (Ref 31). The specific equilibrium that determines the size and shape of the voxel is between the capillary forces in the powder and surface tension in the binder, and it affects the surface finish and resolution of the print.

After deposition of the binder into the powder bed, heat can be applied to the layer to slightly dry the binder, which commonly means boiling off some of the solvent carrier in the binder system. Too little heat on a layer can leave the layer too wet, which results in the moisture wicking into the layer above and contacting the roller, creating a sticky spot on the roller, which can affect the smoothness of the layer. However, the level of heat must be finely tuned, because too much heat can leave the layer too brittle or cause the edges of the layer to curl upward and get caught on the roller, either ruining the build or, at the least, creating a defect in the print. For two-part binder systems in sand printing, the polymer component is coated on the particles and the solvent is jetted from the printhead, and the two react to bond the particles together without needing a heater.

Curing and Depowdering

After printing, the entire powder bed is moved to a curing oven and heated to a temperature sufficient to boil off the solvent, usually around 200 °C. Some binder jetting machines have extractor tools to remove the entire powder bed from the machine without disturbing the print, while others have a removeable build box that detaches from the machine and enables easy transfer of the powder bed to curing or postprocessing. Oven curing time depends on the size of the print, with prints less than a few cubic inches taking one to two hours and larger prints of several hundred cubic inches taking at least eight hours. In addition to the time at temperature for curing, a cool down time is needed before parts can be extracted from the powder bed. Typically, curing is done overnight. For other binder systems such as the two-part furan system used in sand printing for castings, no post-curing is necessary as the part cures during the print itself.

The most involved portion of the binder-jet cycle is depowdering, which comes after the curing step (Fig. 2b). This is the stage in which each part is physically extracted from the build volume by hand and carefully brushed. At this stage, the parts are considered "green," meaning they are loosely bound and somewhat fragile (with strength similar to that of a piece of chalk), so removal from the powder bed without breakage can be challenging for some printed geometries. Techniques to fully de-powder parts include using brushes and low-pressure compressed air to remove loose powder from the sides of the part.

For sand printing, mold pieces can be very large, up to a meter in each dimension, so handling prints is usually accomplished using a forklift or overhead crane. Lifting features such as gaps for forklift tines should be designed into the print for easier handling. Depowdering sand molds occurs much the same way as previously described, just on a larger scale. Once de-powdered, printed sand molds can be used immediately for metal casting.

Sintering

A binder jet printed part must undergo a sintering or infiltration cycle to achieve desirable mechanical properties. Parts that are to be post-processed to full density without an infiltrating component are set in a crucible either on top of a fixture called a "setter" or buried in setter media such as aluminum oxide (a list of setter media can be found in Ref 32). Parts are heated to a sintering temperature below the melting point of the material, but high enough that the particles start to coalesce. Thus, sintering is the process of fusing particles using thermal energy. The advantage of sintering single alloys to full density in this manner is that more desirable material properties can be achieved compared with most metal-matrix composites (MMCs). However, a major drawback of sintering printed single alloy green parts is the shrinkage and distortion that occurs as the particles draw closer together. The shrinkage and distortion can mostly be controlled and/or predicted for small parts, such as those smaller than a golf ball (or rather, the scrap rate due to the variation in shrinkage and distortion is acceptable for small parts). Overall, sintering is the focus of much research, as many challenges must be overcome in geometry control, grain growth, and others.

Different types of sintering can be used to densify powder parts, including solid-state, liquid-state, and super-solidus liquid-phase sintering (Ref 32). Solid-state sintering (SSS) is a lower-temperature process that avoids forming any liquid phase. Because no liquid phase is present in SSS, the effects of gravity on the powder are small, and sagging during the sintering cycle is minimized. However, SSS is generally slow, and for some materials that do not sinter readily, it does not guarantee full density. Fine powders (< 15 μm) are best suited for SSS. However, because of their increased surface area, binder jetting equipment must be adapted to spread and handle these powders safely. Liquid-phase sintering (LPS) uses a significant amount of liquid phase around the particles. With the liquid outer shell, LPS can rely on a much stronger force (surface tension) to pull powder particles together. Using the surface tension of the molten metal film to densify powders is much faster than SSS, but parts are more prone to distortion due to gravity. Some researchers look to super-solidus liquid-phase sintering (SLPS) to strike a balance between speed and distortion. SLPS has a small fraction of liquid phase compared with LPS, but more liquid phase than SSS, which means distortion can be minimized while densification rates can be maximized.

A major drawback to all types of sintering is distortion due to varying shrinkage rates within the part. When a part is being sintered to full density, it typically goes from around 50% dense by volume to nearly 100% dense, which means the dimensional shrinkage is on the order of 20%, as illustrated in Fig. 3 (Ref 34). This means that not only size change must be considered, but also the distortion in the geometry from the significant movement of matter during sintering. In other words, the forces that drive the part to sinter to full density can act unevenly throughout the part, causing sintering distortion. This phenomenon is common to all powder metallurgy (PM) processes, and forces simplicity in design for large binder-jet parts, as well as the leveraging of strategies like using sintering setters to drive the final part shape (Ref 32, 35).

For printed parts that are to be infiltrated instead of sintered (such as the previously mentioned steel powder infiltrated with bronze), shrinkage is avoided completely. In the crucible, printed parts are connected to a runner, which drops into a well in the crucible that holds the infiltrating feedstock. As the crucible and its contents are heated in the furnace, the polymer binder burns off and the infiltrant becomes molten. Because the chemistry between the two materials is favorable for wetting (as well as other properties that will be discussed later) (Ref 36), the infiltrant wicks into the porous steel print using capillary forces. This results in filling the void space between the particles and bringing the part to full density. The final part is a metal-matrix composite with the infiltrant being the metal matrix that surrounds the printed particles.

In summary, furnace cycles are used to transform parts created by binder jet printing from low-density preforms to fully dense components either by sintering or infiltration. Different sintering strategies can be used depending on the material and the desired shape retention, and infiltration can be used when a metal-matrix composite is desired.

Advantages

As with any manufacturing process, binder jetting has unique advantages and disadvantages

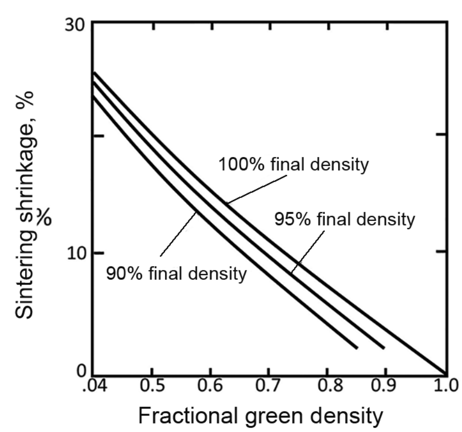

Fig. 3 Sintering shrinkage as a function of green density. Adapted from Ref 33

in terms of the types of artifacts that can be produced and at what price point. Disadvantages of the process include warpage and/or grain growth during sintering, fragility of the printed preforms, and a relatively unexplored material space. However, overall, binder jetting is preferred over laser powder bed fusion, because it inherently produces isotropic grain structures; is flexible in terms of what materials can be net shaped; has a high throughput, and, therefore, lower cost per part; and can produce very fine features without adding more time to the print.

Isotropic Properties

Isotropic refers to the uniformity of a physical or mechanical property when measured in any direction. For additive parts, nonisotropic properties typically mean that the strength of the material parallel to the build layer plane is different from the strength perpendicular to the build layer plane. The difference in strength is commonly due to the repeated melting and solidification that occurs in each layer with AM processes like directed energy deposition, powder bed fusion, and melt extrusion. Because the layer-wise shaping during the binder jet print occurs at low temperatures, the layer-wise effect is insignificant compared with that of the previously mentioned processes. Further, because thermal fusing occurs in a sintering furnace and printed objects are heated more or less evenly, the grain structure throughout the part develops evenly throughout the part and gives the part isotropic properties. The difference in microstructure between binder jetting and laser powder bed fusion can be seen in Figs. 4 and 5, respectively.

Low Cost, High Throughput

Throughput is a crucial factor when considering any piece of manufacturing equipment, and typically AM systems cannot compete with the economies of scale in mass production manufacturing (Ref 38). Thus, the most common investors in AM equipment and manufacturing research are in high-value markets like aerospace, medical, and high-end automotive (Ref 39). However, with binder jetting, the potential to compete with mass production exists at least for now in MIM replacement parts up to quantities of 30,000 (Ref 40). The reason that binder jetting can produce parts so economically stems from major characteristics such as (Ref 8-10):

- Multiple parts can be printed simutaneously in the layer without adding to print time
- Parts can be stacked densely on top of each other
- Parts are printed, cured, de-powdered, and sintered in large batches

Using ink-jet printing as the shaping technique gives binder jetting a distinct speed advantage over other AM processes, because printheads can be designed with hundreds of nozzles and operate at frequencies of around 10 kHz (Ref 41), resulting in the ability to shape a large layer of powder within a few seconds. Thus, with binder jetting, multiple parts can be printed simultaneously without adding to print time, creating an economy of scale in the process. By comparison, powder bed fusion or extrusion technologies have single-point deposition or melting strategies, which means speed is limited by how fast the machine can raster the beam or extrusion nozzle. Also, unlike powder bed fusion and extrusion technologies that use support structures to anchor the part to the build plate, binder-jet parts can be stacked on top and around each other in close proximity in the build bed, meaning that for each print, the job box can be stacked to the top with hundreds of parts. This increases the economies of scale, because not only can multiple parts be printed in a layer, but also, multiple layers of parts can be printed in one job box. Binder jetting is poised to compete with mass production manufacturing, because each step of the process (printing, curing, and sintering) can be performed in large batches. Thus, with strategic placement of parts in the build bed and in the furnace, large volumes of parts can be processed in a single cycle.

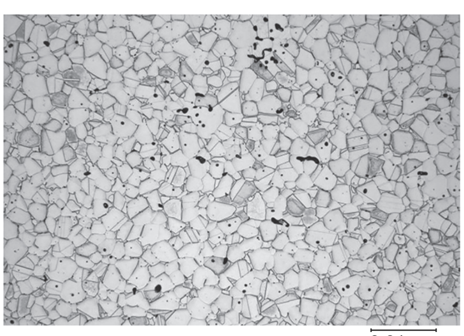

Fig. 4 Microstructure of a binder jet part showing isotropic grain structure. Source: Ref 37

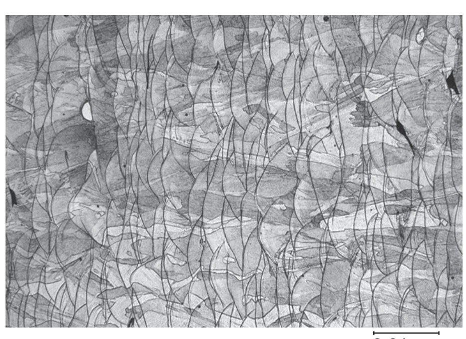

Fig. 5 Microstructure of laser powder bed fusion build showing distinct nonisotropic weld patterns. Source: Ref 37

Material Flexibility

Most metal AM processes are highly constrained in terms of what feedstocks are viable. For example, laser powder bed fusion requires that metal powder feedstocks have a relatively prescribed size distribution and shape and a certain level of compatibility with the laser beam itself. Further, the weldability and thermal conductivity of the powder feedstock significantly affect the ability to form a controllable melt pool. However, for binder jetting, most powder feedstocks can at least be net shaped (although not necessarily sintered or infiltrated to full density). This is due to the spreading mechanism, the binder system, and the postprocessing strategy. Because the spreading mechanism in binder jetting is a CRR, a wider range of powder size distributions and particle shapes can be effectively spread. This is because the CRR creates movement in the powder and enables spreading even the most jagged powders such as carbides just as easily as highly engineered spherical metal powders. The binder system itself adheres to virtually any material, so if a powder can be spread in a layer, it can be shaped with the binder. Because postprocessing of binder-jet parts involves sintering, many techniques exist to densify a material that is net shaped with binder jetting. Thus, the limitations of a laser for printing high-temperature materials such as carbides and oxides are overcome by binder jetting. Further, as advanced sintering techniques like hot isostatic pressing (HIP) become more prevalent, sintering of binder-jet parts can result in properties superior to those of parts produced by conventional manufacturing.

Resolution at Little Cost to Speed

Just as an ink-jet printer can create intricate fonts on the same page as a simple block diagram, binder jetting can create high-resolution features in the print layers without slowing down the printing process. This means that value can be added to products by including fine features without significantly adding to the cost of the process. This feature is especially important in the MIM industry, which is limited by molding technology as to what features can be produced. For example, the highly detailed MIM-size medieval castle in Fig. 6 can be created via binder jetting, but many of the features of the shape (such as multiple out-of-plane spires and the concave buttresses) cannot be molded. For industrial applications (e.g. heat exchangers), intricate geometries can be imagined that would add functionality to the part, but cannot be made using molding processes. However, it should be noted that for these high-resolution prints, the layer size of the print must be reduced, which does add to print time. However, the ability to print and process many of these parts in large batches remains the same.